Supplementary Information (SI) for Chemical Communications.

Supplementary Information

Surface Ni-O-Co Sites in Cube-Shaped Ni-Co_3O_4 Spinel Oxides for Boosting Soot Oxidation

Linsheng Xu,[a] Haoqi Guo,[a] Wen Cao,[b] Jing Xiong,[a] Yaxiao Ma,[a] Baolong Cui,[a] Zekai Cui,[a] Hao Guo,[a] Peng Zhang,[a] and YuechangWei,*[a]

[a] State Key Laboratory of Heavy Oil Processing, Key Laboratory of Optical Detection Technology for Oil and Gas, China University of Petroleum, Beijing 102249, China

[b] China Tobacco Shaanxi Industrial Co., Ltd., Xi'an 710065, China.

* Corresponding author: weiyc@cup.edu.cn (Y. Wei)

Methods

Chemicals

Cobalt(II) nitrate hexahydrate [$Co(NO_3)_2·6H_2O$], nickel(II) nitrate hexahydrate [$Ni(NO_3)_2·6H_2O$] and sodium hydroxide [NaOH] purchased from Aladdin Ltd. (Shanghai, China), were used as received without further purification.

Catalyst preparation

Preparation of cube-shaped Co_3O_4.

$Co(NO_3)_2·6H_2O$ was dissolved in 10 mL of deionized water to yield a precursor solution with a metal cation concentration of 2 mol/L. NaOH was dissolved in 10 mL of deionized water to yield a solution with a metal cation concentration of 2 mol/L. The solution of NaOH was slowly added dropwise to the precursor solution and stirred continuously for 40 minutes to form a slurry. The slurry was transformed into a Teflon-lined stainless-steel autoclave and hydrothermally treated at 180 ^oC for 12 h to obtain black precursor. After being cooled to room temperature, the obtained precipitate was collected by centrifugation and washed with deionized water and ethanol, and then dried overnight at 50 ^oC. The black precursor was annealed at 500 ^oC for 4 hours in air to obtain cube-shaped Co_3O_4.

Preparation of Ni_x-Co_3O_4 catalysts. Different qualities of $Ni(NO_3)_2·6H_2O$ were dissolved in deionized water to prepare solutions with Ni ion concentrations of 0.5, 1.0, and 2.0 mol L^{-1}. The black precursor of 0.1g was annealed at 500 ^oC in a muffle furnace. After annealing for 3 hours, the precursor is removed from the furnace and immediately quenched by pouring it into 50 mL pre-prepared Ni solutions of 0 (deionized water), 0.5, 1.0, and 2.0 mol L^{-1} to obtain water-Co_3O_4, $Ni_{0.5}$-Co_3O_4, $Ni_{1.0}$-Co_3O_4 and $Ni_{2.0}$-Co_3O_4 catalysts respectively.

Characterizations

Powder X-ray diffraction (XRD) patterns were obtained by a diffractometer (Bruker D8 advance) over the 2θ range from 5 to 90° with a 5° min^{-1} scanning rate using Cu-Kα radiation to obtain the phase structure of all as-prepared catalysts. The Ni/Co content of catalysts was measured by using inductively coupled plasma optical emission spectrometry (ICP-OES). Scanning electron microscopy (SEM), images were obtained by Quanta 200F. Transmission electron microscope (TEM) and mapping images were obtained by FEI Tecnai G2 F20 transmission electron microscope. Raman spectra of all catalysts were measured on an inVia Reflex-Renishaw spectrometer with an excitation wave-length of 532 nm. The temperature programmed reduction of hydrogen (H_2-TPR) was carried out on an Automatic Chemisorption Analyzer. The catalysts were pretreated with N_2 at 350 °C for 30 min before test. After cooling to room temperature, H_2-TPR was conducted with flowed the gaseous contained H_2 (7 vol%) balanced with N_2 (30 mL min^{-1}). And the temperature range of the H_2-TPR is 50 to 900 °C with a ramp rate of 10 °C min^{-1}. The temperature-programmed oxidation of NO (NO-TPO) was carried out on a fixed-bed tubular quartz reactor, and the products can be detected by online FT-IR. The catalysts were pretreated with N_2 at 100 °C for 30 min before test. After cooling to room temperature, NO-TPO was conducted with flowed the gaseous contained O_2 (5 vol%) and NO (0.1 vol%) balanced with N_2 (50 mL min^{-1}). And the temperature range of the NO-TPO reaction is 50 to 500 °C with a ramp rate of 2 °C min^{-1}. Temperature-programmed desorption of O_2 (O_2-TPD) measurements were conducted on a fixed bed and the desorption signal of oxygen was recorded with an online mass spectrometer apparatus (HIDEN DECRA). 0.1 g fresh catalyst was put into a quartz tube reactor and pretreated in an Ar flow with a flow rate of 50 mL min^{-1} for 30 min at 300 °C at a heating rate of 10 °C min^{-1}. After cooling to room temperature, the catalyst was exposed to high-purity O_2 with 50 mL min^{-1} for 30 min. Then, the stream was switched to Ar to purge for 1 h. Finally, the heating rate was set to be 10 °C min^{-1} with a 50 mL min^{-1} Ar flow. Temperature programmed surface reaction of CO (CO-TPSR) was performed on a fixed-bed tubular quartz microreactor. 0.1 g catalyst was pretreated with pure oxygen at 350 °C for 30 min. After being cooled to ambient temperature under pure argon, a 10 vol% CO/Ar gas stream was introduced (50 mL min-1). The temperature was increased from room temperature to 900 °C with a heating rate of 10 °C min^{-1}. The outlet gases were monitored with an online mass spectrometer apparatus (HIDEN DECRA). The CO_2 signal (m/z = 44) and CO signal (m/z = 28) were monitored during the surface reaction without gaseous oxygen supply. The surface element valence state was detected by X-ray photoelectron spectra (*XPS*, XPSPHI−1600 ESCA spectrometer), calibrated using a C *1s* binding energy of 284.8 eV. *In situ* diffuse reflectance infrared Fourier transforms (*in situ* DRIFT) spectra were carried on a Bruker FT-IR spectrometer (TENSOR II) equipped with a liquid nitrogen-cooling mercury-cadmium-telluride (MCT) detector. The catalyst was added into high-temperature IR cell with ZnSe window, and heated in N_2 flow at 200 °C for 30min to remove adsorbed H_2O and other materials. After cooling down to 50 °C with N_2 atmosphere, the background spectrum was recorded. Finally, the gas to be measured were fed into cell at a flow rate of 50 mL min^{-1}. IR spectra of simultaneous NO and CH_4 oxidation were recorded in a flow of 0.2 vol %NO/5 vol% O_2/N_2 balance (50 mL min^{-1}) under heating from 30 to 450 °C.

Catalytic activity tests

The catalytic activity of all as-prepared catalysts for soot oxidation was evaluated by soot temperature programmed oxidation (soot-TPO) on a continuous flow micro-reactor constituted of a quartz tube of 8 mm of the outside diameter. The reactor was heated from 150 to 650 °C at a heating rate of 2 °C min^{-1} in a stream of 0.2 vol% NO and 5 vol% O_2 balanced with N_2 at a total flow rate of 50 mL min^{-1}. The catalyst (0.1 g) and soot (0.01 g) were fully mixed using a spatula for 10 min to simulate loose contact. The concentration of CO and CO_2 in the outlet gas was monitored by online gas chromatography (GC 9890B, Shanghai) with a flame ionization detector (FID). The catalytic activity was evaluated and compared in terms of T_{10}, T_{50}, and T_{90}, corresponding to the temperature at which 10%, 50%, and 90% of soot is converted. The selectivity of CO_2 formation (S_{CO2}) was defined as the CO_2 outlet concentration (C_{CO2}) divided by the sum of CO_2 and CO outlet concentration. $S_{CO2}{}^{m}$ was denoted as the S_{CO2} at which the C_{CO2} value was the maximum. The CO_2 selectivity (S_{CO2}) was measured according to the following equation (1):

$$S_{CO2}(\%) = \frac{[CO_2]_{out}}{[CO]_{out} + [CO_2]_{out}} \times 100\% \quad (1)$$

Here, the $[CO_2]_{out}$ and $[CO]_{out}$ represent the outlet CO_2 and CO concentration, respectively.

he apparent activation energy of soot oxidation was measured by the single heating rate method (Coats-Redfern integral method) according to the equation (2):

$$\beta\frac{d\alpha}{dT} = k(T)f(\alpha) \rightarrow \beta\frac{d\alpha}{dT} = A \times \exp\left(-\frac{E_a}{RT}\right)f(\alpha) \quad (2)$$

Where β is the heating rate ($K\ min^{-1}$), α is the soot conversion rate ($\alpha<15\ \%$), T is the reaction temperature (K), k is the reaction rate constant, f(α) is the kinetic expression for the reaction model, $f(\alpha)=(1-\alpha)^n$, where n is the number of reaction stages. A is the pre-finger factor (s^{-1}), E_a is the apparent activation energy ($kJ\ mol^{-1}$), R is the ideal gas constant. Previous studies have shown that the reaction of soot with NO_2 is a one-stage reaction, i.e., n=1. The equation (5) can be obtained:

$$\ln\left[-\frac{\ln(1-\alpha)}{T^2}\right] = \ln\left[\frac{AR}{\beta E_a}\left(1-\frac{2RT}{E_a}\right)\right] - \frac{E_a}{RT} \quad (3)$$

In most cases, $\frac{2RT}{Ea}$ much smaller than 1, and $\ln\left[\frac{AR}{\beta E_a}\left(1-\frac{2RT}{E_a}\right)\right]$ can be regarded as a constant. Then, the apparent activation energy is estimated by plotting $\ln\left[-\frac{\ln(1-\alpha)}{T^2}\right]$ vs 1/RT.

Supplementary Figures

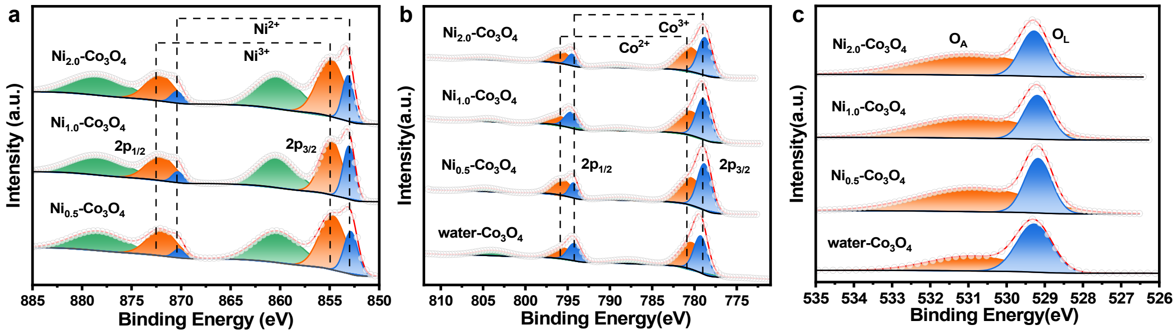

Figure S1. XPS spectra of Ni *2p* (**b**), Co *2p* (**a**), and O *1s* (**c**) over water-Co_3O_4 and Ni_x-Co_3O_4 catalysts.

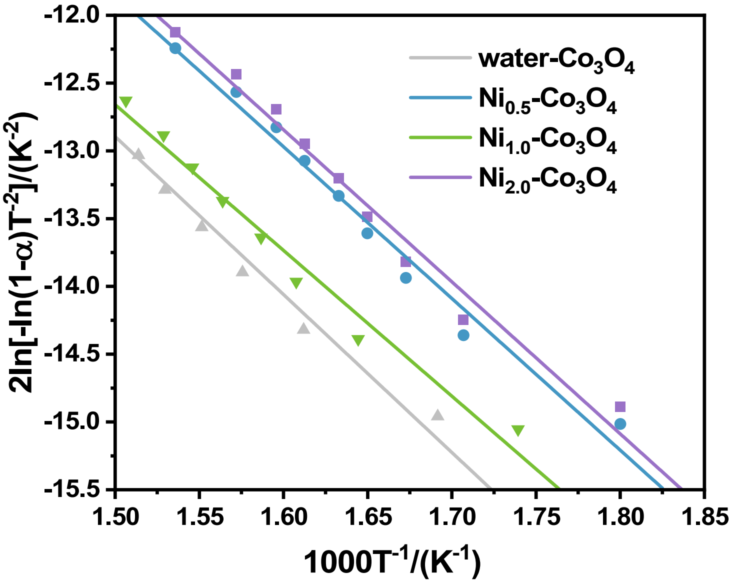

Figure S2. The apparent activation energy of water-Co_3O_4 and Ni_x-Co_3O_4 catalysts for soot oxidation.

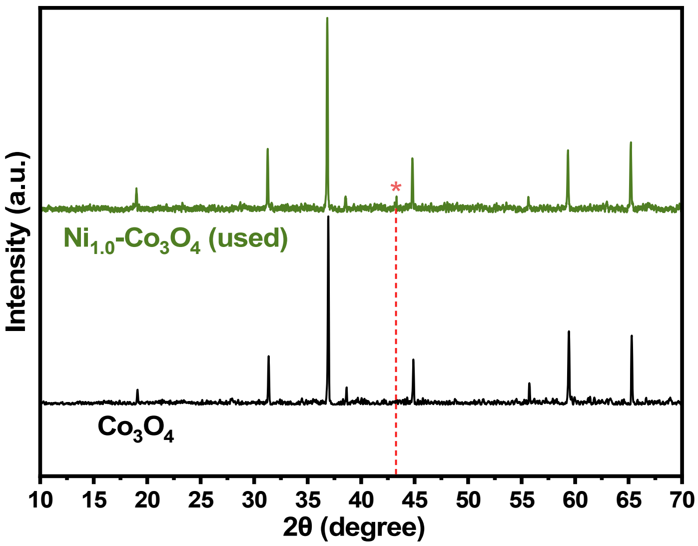

Figure S3. XRD patterns of $Ni_{1.0}$-Co_3O_4 after five cycles tests and fresh Co_3O_4 catalysts.

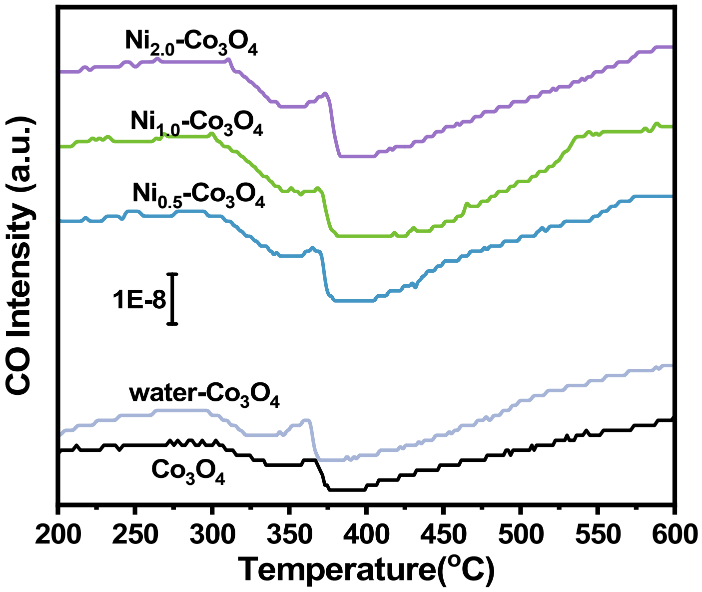

Figure S4. CO signal intensity in CO-TPSR testing of catalysts

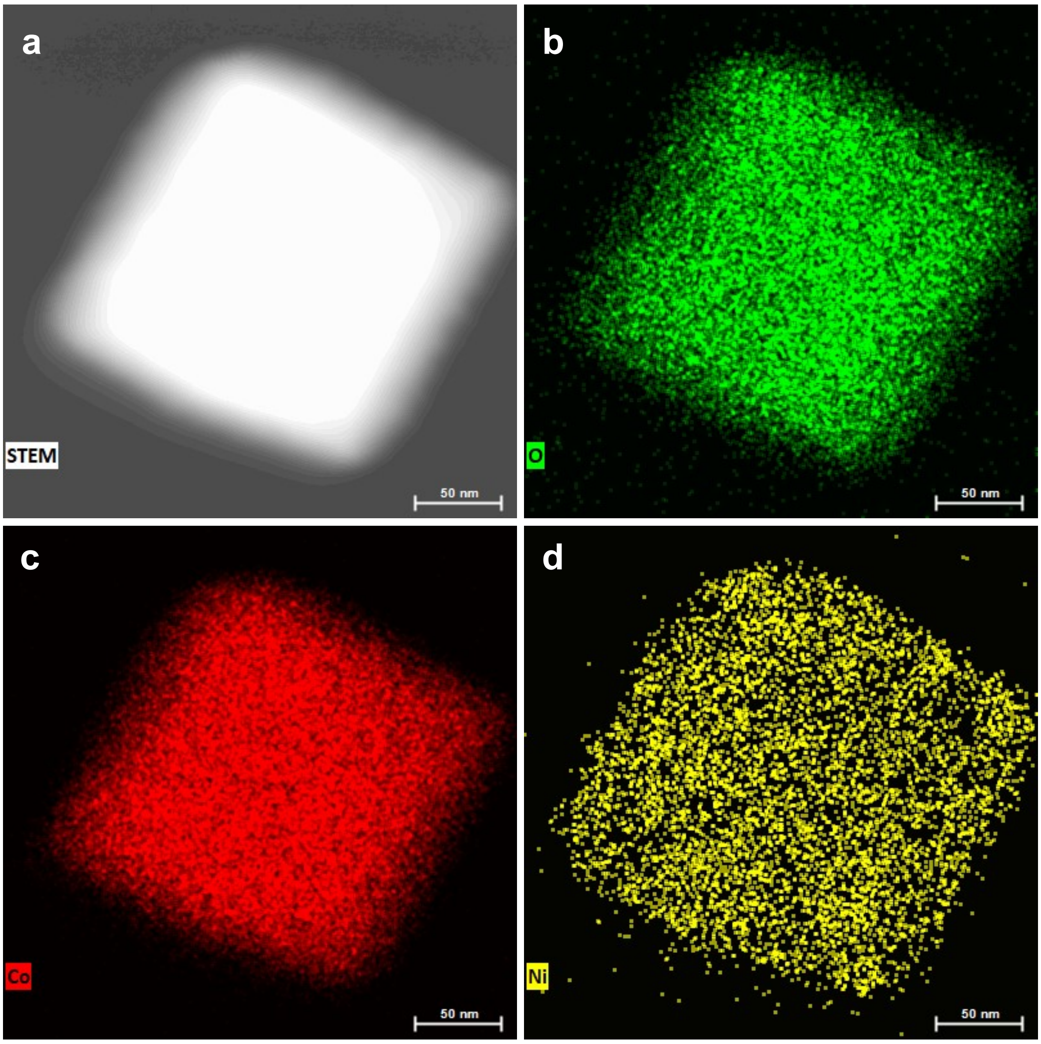

Figure S5. STEM and corresponding element mapping images of cube-shaped $Ni_{1.0}$-Co_3O_4 catalyst.

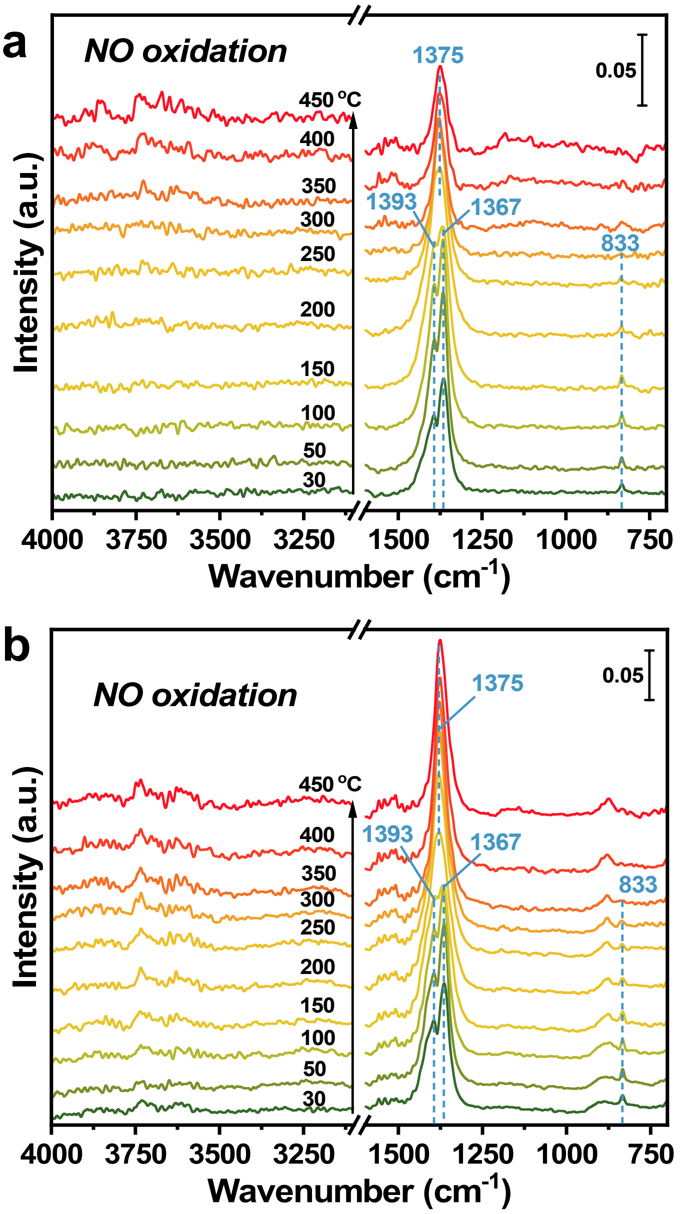

Figure S6. Temperature-dependent *in situ* DRIFT spectra of NO oxidation over (**a**) water-Co_3O_4 and (**b**) $Ni_{1.0}$-Co_3O_4 catalysts.

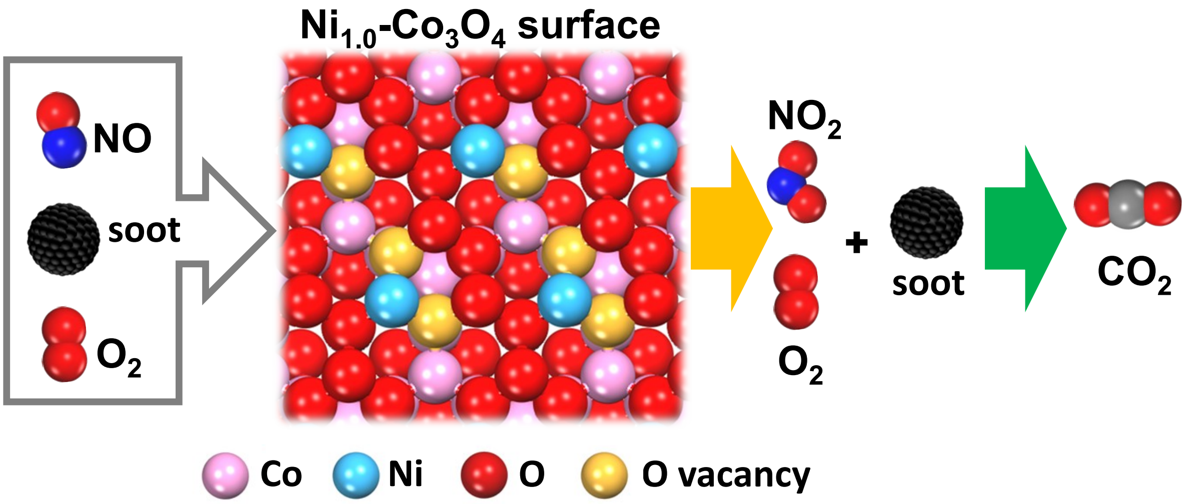

Figure S7. Schematic diagram of NO_x-assisted soot oxidation mechanism on $Ni_{1.0}$-Co_3O_4 catalyst surface.

Supplementary Tables

Table S1. The practical Ni/Co molar ratios in the prepared catalysts determined by ICP-OES

Catalyst	Ni/Co
$Ni_{0.5}$-Co_3O_4	0.124
$Ni_{1.0}$-Co_3O_4	0.222
$Ni_{2.0}$-Co_3O_4	0.386

Table S2. Curve-fitting results of Ni (2*p*), Co (2*p*) and O (1*s*) for catalysts.

	Ni 2*p*			Co 2*p*			O 1*s*		
Catalysts	Ni^{3+}	Ni^{2+}	Ni^{3+}/Ni^{2+}	Co^{3+}	Co^{2+}	Co^{3+}/Co^{2+}	O_A	O_L	O_A/O_L
water-Co_3O_4	-	-	-	0.43	0.57	0.75	0.57	0.43	1.33
$Ni_{0.5}$-Co_3O_4	0.76	0.24	3.12	0.42	0.58	0.72	0.65	0.35	1.85
$Ni_{1.0}$-Co_3O_4	0.71	0.29	2.45	0.46	0.54	0.85	0.67	33.2	2.01
$Ni_{2.0}$-Co_3O_4	0.78	0.22	3.55	0.41	0.59	0.69	0.66	0.34	1.93

Table S3. Catalytic activities of catalysts for soot oxidation.

Catalysts	T_{10} (^{o}C)	T_{50} (^{o}C)	T_{90} (^{o}C)	S_{co2}^{m} (%)	E_a (kJ mol^{-1})
Without catalyst	461	584	648	65.2	-
Co_3O_4	380	447	502	82.2	-
water-Co_3O_4	330	393	443	89.6	96.7
$Ni_{0.5}$-Co_3O_4	302	366	408	99.1	93.0
$Ni_{1.0}$-Co_3O_4	282	339	378	99.3	89.4
$Ni_{2.0}$-Co_3O_4	318	381	418	98.9	93.3

Table S4. Comparison of Co-based oxides system for soot oxidation: synthesis method, reaction condition, catalytic activity (T_{50}) and corresponding reference.

Catalysts	**Synthesis method**	**Reaction condition**	**T_{50} (^oC)**	**Ref.**
$Ni_{1.0}$-Co_3O_4	Quenching method	2000 ppm NO/5% O_2/N_2, 50 mL min^{-1}	339.3	This work
3DOM-$NiCo_2O_4$	Carboxy-modified colloidal crystal templating method	1000 ppm NO/5% O_2/N_2, 300 mL min^{-1}	379	1
3DOMM $PdCo_2O_4$/CZO	Evaporation-induced self-assembly and colloidal crystal templates methods	2000 ppm NO/5% O_2/Ar, 50 mL min^{-1}	367	2
$Ag/Co_3O_4@CeO_2$	Hydrothermal, chemical precipitation and impregnating methods	500 ppm NO/5% O_2/N_2, 500 mL min^{-1}	395	3
K-Co_3O_4 nanowire	Hydrothermal and facile wet impregnation methods	600 ppm NO/5% O_2/N_2, 100 mL min^{-1}	324	4
3DOM $La_{0.9}K_{0.1}CoO_3$	Carboxy-modified colloidal crystal templates method	2000 ppm NO/5% O_2/Ar, 50 mL min^{-1}	398	5
3DOM $Pt@CoO_x/Al_2O_3$	colloidal crystal template and GBMR/P methods	2000 ppm NO/5% O_2/Ar, 50 mL min^{-1}	357	6
0.5%Pd-1%Co/Beta	Impregnation method	1000 ppm NO/10% O_2/N_2, 500 mL min^{-1}	398	7
5%Cs/1%Co/MnO_x	Hydrothermal, wetness impregnation method	1000 ppm NO/10% O_2/N_2, 300000 mL g^{-1} h^{-1}	371	8

CoO_x/TiO_2	Sequential deposition–precipitation with urea method	250 ppm NO_x/50% Air/N_2, 100 mL min^{-1}	358	9
Co/Ce-YSZ	Impregnated and redox-aging cycle methods	500 ppm NO/5% O_2/N_2, 500 mL min^{-1}	509	10

Reference

1. M. Zhao, J. Deng, J. Liu, Y. Li, J. Liu, Z. Duan, J. Xiong, Z. Zhao, Y. Wei, W. Song and Y. Sun, *ACS Catal.*, 2019, **9**, 7548-7567.
2. J. Xiong, Q. Wu, X. Mei, J. Liu, Y. Wei, Z. Zhao, D. Wu and J. Li, *ACS Catal.*, 2018, **8**, 7915-7930.
3. X. Wang, B. Jin, R. Feng, W. Liu, D. Weng, X. Wu and S. Liu, *App. Catal. B: Environ.*, 2019, **250**, 132-142.
4. C. Cao, L. Xing, Y. Yang, Y. Tian, T. Ding, J. Zhang, T. Hu, L. Zheng and X. Li, *App. Catal. B: Environ.*, 2017, **218**, 32-45.
5. J. Xu, J. Liu, Z. Zhao, C. Xu, J. Zheng, A. Duan and G. Jiang, *J. Catal.*, 2011, **282**, 1-12.
6. Q. Wu, M. Jing, Y. Wei, Z. Zhao, X. Zhang, J. Xiong, J. Liu, W. Song and J. Li, *App. Catal. B: Environ.*, 2019, **244**, 628-640.
7. M. Wang, C. Duan, M. Liu, Z. Chen, J. Cai, Y. Zhang, Y. Yu and W. Shan, *Small*, 2025, **21**, 2501373.
8. M. Wang, Y. Zhang, Y. Yu, W. Shan and H. He, *Environ. Sci. Technol.*, 2021, **55**, 240-248.
9. N. S. Portillo-Vélez and R. Zanella, *Chem. Eng. J.*, 2020, **385**, 123848.
10. M. P. Yeste, M. Á. Cauqui, J. Giménez-Mañogil, J. C. Martínez-Munuera, M. Á. Muñoz and A. García-García, *Chem. Eng. J.*, 2020, **380**, 122370.